Astron. Astrophys. 332, 732–738 (1998)

ASTRONOMY AND ASTROPHYSICS

Resonance scattering of Lyman alpha from interstellar hydrogen

Mats Braskén and Erkki Kyrölä

[1] Åbo Akademi University, Department of Physics, Porthansgatan 3, FIN-20500 Åbo, Finland
[2] Finnish Meteorological Institute, Geophysical Research Division, P.O. Box 503, FIN-00101 Helsinki, Finland

Received 20 June 1996 / Accepted 12 December 1997

Abstract. We derive a set of new line-of-sight (LOS) integrals and phase functions for the resonance scattering of unpolarized Lyman α light in the optically thin medium limit. To explicitly show the approximations done, and to indicate the range of validity of previously published formulas, we start by treating the general theory of resonance scattering. For broad band Lyα and a hot gas the resulting LOS integral can be evaluated analytically. This is the case for Lyα light from the sun scattering off neutral interstellar hydrogen. The ground state populations of the hydrogen atom will effect the value of the scattered intensity. Two population distributions are considered: a thermal equilibrium population and a population established by the atom-light interaction.

Key words: atomic processes – scattering – ISM: general – polarization

1. Introduction

Resonantly scattered Lyman α (Lyα) light provides an important probe for studying the distribution and properties of the neutral, atomic hydrogen in the local interstellar medium. The scattered light carries information about the column density and velocity distribution of the hydrogen atoms. Indirectly, the scattered light also gives information about the spatial and temporal variations of the solar wind. To retrieve this information, however, theoretical expressions for the scattered intensity are of essence.

Although the quantum theory of resonant light scattering has been known since the early years of quantum mechanics (Weisskopf 1931; Breit 1933; Hamilton 1947), expressions for the angular dependence of the scattered intensity (or phase functions) are not common in the literature (two exceptions are Brandt & Chamberlain 1959 and Chamberlain 1990). The phase functions given by Brandt and Chamberlain are, however, presented without explicitly showing the connection with theory and without clearly stating the approximations used in the derivation. It is therefore the aim of this article to, starting from the quantum theory of resonance scattering, derive a general expression for the measured intensity and apply it to the scattering of unpolarized Lyα light from neutral hydrogen. For the special case of broad band light and a hot scattering gas it is possible to obtain a closed form expression for the line-of-sight (LOS) integral, in the optically thin medium limit. This special case is valid for the important case for Lyα from the sun, FWHM ~ 1 Å, scattering from interstellar neutral hydrogen, T ~ 8000 K (values are from Holzer 1977).

We will give the scattered intensity for two different level structures of hydrogen; with and without hyperfine structure, and for two sets of ground state populations; thermal and non-thermal populations. The latter populations dominate close to the sun where the induced photon absorption rate greatly exceeds the atomic collision rate. Using the formula for the scattered intensity we will finally derive the degree of polarization and phase functions.

Send offprint requests to: M. Braskén

2. Theory

The rate of a resonance scattering process where $n_{\mathbf{k}\sigma}$ photons of frequency $\omega_{\mathbf{k}}$ and polarization $\hat{e}_\sigma$ are absorbed, while photons of frequency $\omega_{\mathbf{q}}$ and polarization $\hat{e}_{\overline{\sigma}}$ are emitted, is given by

$$W = \frac{\pi e^4 \omega_{\mathbf{k}} \omega_{\mathbf{q}} n_{\mathbf{k}\sigma}}{2\epsilon_0^2 V^2 \hbar^2} \sum_f \left| \sum_m \frac{\langle f| \hat{e}_{\overline{\sigma}} \cdot \hat{\mathbf{r}} |m\rangle \langle m| \hat{e}_\sigma \cdot \hat{\mathbf{r}} |i\rangle}{\omega_{\mathbf{k}} - \omega_{mi} - i\frac{\Gamma_m}{2}} \right|^2 \delta(\omega_{\mathbf{k}} - \omega_{\mathbf{q}}), \quad (1)$$

where $|i\rangle, |m\rangle$ and $|f\rangle$ are the initial, intermediate, and final atomic states. Eq. (1) is a special case of the Kramers-Heisenberg formula of dispersion (Louisell 1973).

For an atom moving relative to the emitting light source the center of mass $\mathbf{R}$ of the atom will become time-dependent. Denoting the velocity of the atom relative to the source and the observer by $\mathbf{v}$, the effect of a moving center of mass position is equivalent to making the following two substitutions in Eq. (1)

$$\begin{aligned} \omega_{\mathbf{k}} &\longrightarrow \omega_{\mathbf{k}} - \mathbf{v} \cdot \mathbf{k} \\ \omega_{\mathbf{q}} &\longrightarrow \omega_{\mathbf{q}} - \mathbf{v} \cdot \mathbf{q}. \end{aligned} \quad (2)$$

These substitutions give the Doppler shift in the absorbed and emitted light frequencies due to the relative motion of the atom.

The response of an atom to an incoherent light source, containing a distribution of different photon frequencies, is obtained

by summing Eq. (1) over all incoming frequencies. If we denote the flux of photons in mode $\mathbf{k}\sigma$ by $\phi_{\mathbf{k}\sigma} \equiv n_{\mathbf{k}}c/V$ then due to the fact that the modes are very closely spaced $\phi_{\mathbf{k}\sigma}$ can be replaced by a continuous distribution $\phi(\omega)$ (ϕ has the units m^{-2} s^{-1} Hz^{-1}). Integrating over all incoming frequencies the total transition rate is

$$W_t = \frac{\pi e^4 \omega_{\mathbf{q}}^2}{2\, c\epsilon_0^2 V \hbar^2} \phi\left(\frac{\omega_{\mathbf{q}} - \mathbf{v}\cdot\mathbf{q}}{1 - \frac{\mathbf{v}}{c}\cdot\hat{e}_{\mathbf{k}}}\right) \sum_f \left| \sum_m \frac{\langle f|\, \hat{e}_{\overline{\sigma}}\cdot\hat{\mathbf{r}}\,|m\rangle\, \langle m|\, \hat{e}_{\sigma}\cdot\hat{\mathbf{r}}\,|i\rangle}{\omega_{\mathbf{q}} - \omega_{mi} - \mathbf{v}\cdot\mathbf{q} - i\frac{\Gamma_m}{2}} \right|^2 . \quad (3)$$

In Eq. (3) we have only retained the Doppler shift in the argument of ϕ and in the resonance profile, as there small shifts in frequency can become critical. The finite frequency resolution $d\omega_{\mathbf{q}}$ of the photon detector that measures the scattered light, is taken into account by using the density of photon states: $V d\Omega_{\mathbf{q}} \omega_{\mathbf{q}}^2 d\omega_{\mathbf{q}}\, (2\pi c)^{-3}$. Eq. (3) then becomes

$$W_t = \frac{\alpha^2 \omega_{\mathbf{q}}^4 d\omega_{\mathbf{q}} d\Omega_{\mathbf{q}}}{c^2}\, \phi\left(\overline{\omega}_{\mathbf{q}}(\mathbf{v})\right) \sum_f \left| \sum_m \frac{\langle f|\, \hat{e}_{\overline{\sigma}}\cdot\hat{\mathbf{r}}\,|m\rangle\, \langle m|\, \hat{e}_{\sigma}\cdot\hat{\mathbf{r}}\,|i\rangle}{\omega_{\mathbf{q}} - \omega_{mi} - \mathbf{v}\cdot\mathbf{q} - i\frac{\Gamma_m}{2}} \right|^2 , \quad (4)$$

where we have introduced the fine structure constant α ($\approx 1/137$) and denoted the shifted argument of ϕ by $\overline{\omega}_{\mathbf{q}}(\mathbf{v})$. Expression (4) gives the probability per unit time that a photon having a frequency $\omega_{\mathbf{q}}$ within the interval $d\omega_{\mathbf{q}}$ is scattered into the solid angle $d\Omega_{\mathbf{q}}$ surrounding $\mathbf{q}$.

2.1. LOS integral

Eq. (4) refers to the scattering from a single atom. In any real situation there is allways a large number of scattering atoms present. In what follows we will assume that a photon is only scattered once on its way to the observer (the thin medium approximation). Referring to Fig. 1 the number of atoms at a distance s from the observer within the solid angle $d\Omega$ equals $N = n(s)s^2\, ds\, d\Omega$, where $n(s)$ is the number density at point s. The dependence of the photon flux on the distance $\mathbf{r}(s)$ to the light source is in the absence of absorption $\phi_0 r_0^2/r^2(s)$, where ϕ_0 is the flux at the position $\mathbf{r}_0$ of the observer and where we assumed a point source. As the scattered intensity falls off as s^{-2}, the s^2 term in the expression for N will cancel. We take the velocities of atoms at $\mathbf{r}(s)$ to be distributed according to the normalized velocity distribution $F(\mathbf{v}, s)$:

$$F(\mathbf{v}, s) = \frac{f(\mathbf{v}, s)}{\int d\mathbf{v}\; f(\mathbf{v}, s)} , \quad (5)$$

where f is the solution to the appropriate Boltzmann equation for the gas. From f we can also obtain the density n as

$$n(s) = \int d\mathbf{v}\; f(\mathbf{v}, s) . \quad (6)$$

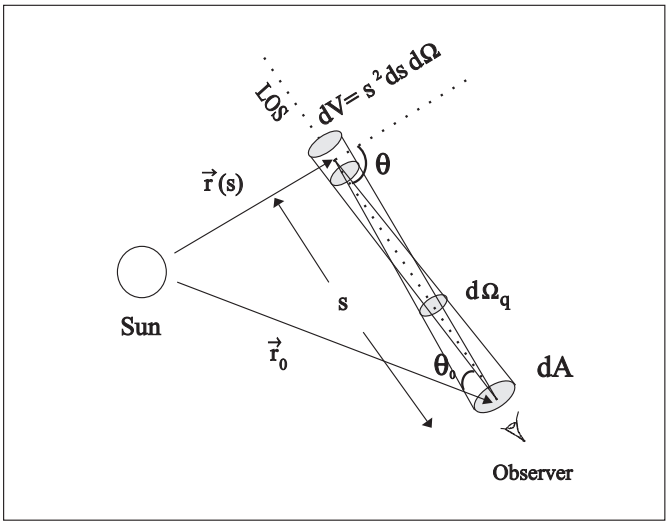

Fig. 1. Definition of the quantities used in deriving the LOS integral.

If we take the fraction of the atoms in the ground state $|i\rangle$ to be ρ_{ii}, then by multiplying Eq. (4) by N and $F(\mathbf{v}, s)$ and integrating over all velocities and along the LOS, we obtain

$$I\ (\omega_{\mathbf{q}}) = \frac{\alpha^2 \omega_{\mathbf{q}}^4 r_0^2}{c^2} d\omega_{\mathbf{q}} d\Omega\, dA \int ds \frac{n(s)}{r^2(s)} \int d\mathbf{v}\; F(\mathbf{v}, s)\, \phi_0\left(\overline{\omega}_{\mathbf{q}}(\mathbf{v})\right) \sum_{i,f} \left| \sum_m \frac{\langle f|\, \hat{e}_{\overline{\sigma}}\cdot\hat{\mathbf{r}}\,|m\rangle\, \langle m|\, \hat{e}_{\sigma}\cdot\hat{\mathbf{r}}\,|i\rangle}{\omega_{\mathbf{q}} - \omega_{mi} - \mathbf{v}\cdot\mathbf{q} - i\frac{\Gamma_m}{2}} \right|^2 \rho_{ii} \quad (7)$$

I($\omega_{\mathbf{q}}$) gives the number of photons counted in a detector of angular opening $d\Omega$, area dA, and frequency resolution $d\omega_{\mathbf{q}}$. It is to be noted that the dipole matrix elements in Eq. (7) contain an implicit s dependence due to the orthogonality relation between the polarization vectors and the photon momentum. Eq. (7) is our main result and one would in general have to resort to numerical calculations to evaluate the integrals. In the next section we will, however, show that for an important special case an analytical solution is possible.

3. Broad band and hot gas limit

To evaluate the scattered intensity we need the dipole matrix elements, ground state populations, some idea about the velocity distribution, and the frequency profile of the incoming light. Lyα corresponds to the 1s-2p transition in hydrogen. If spin-orbit interaction is included the 2p-state will split into a $2P_{1/2}$ and a $2P_{3/2}$ state. A further splitting will occur if we also take into account the hyperfine interaction (Fig. 2). We will restrict our attention to a situation where the following two criteria hold:

1. The $1S_{1/2}$-$2P_{1/2}$ and $1S_{1/2}$-$2P_{3/2}$ transitions receive the same incoming light intensity, thus assuming that the intensity is constant over an 0.005 Å wavelength interval.

2. The width of the Doppler profile is much broader than the natural line width $\Gamma(\approx 10^{-5}$ Å). The Doppler width will, however, be assumed to be smaller than the width of the frequency distribution $\phi_0(\omega)$.

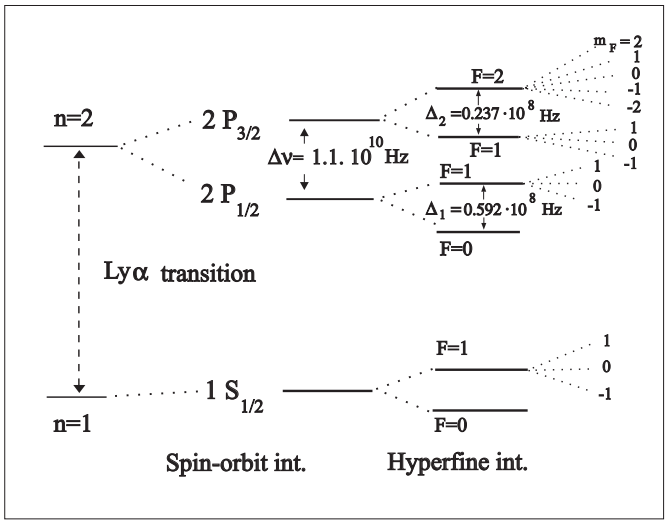

Fig. 2. The structure of the 1s-2p levels in hydrogen. Both spin-orbit and hyperfine interaction will cause a splitting of levels. The degenerate sub-states m_F of the hyperfine levels F is shown together with the size of the frequency separation caused by the two interaction mechanisms.

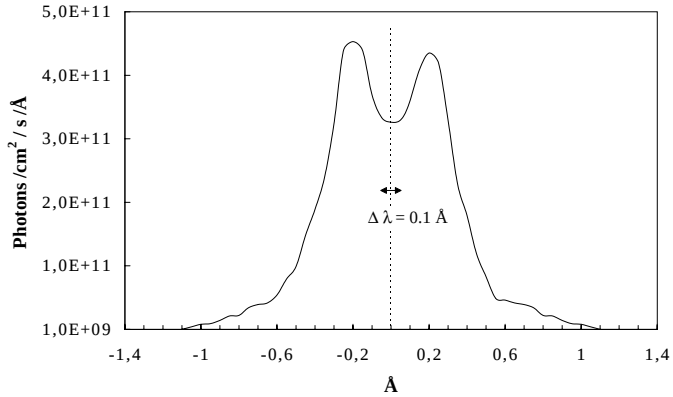

Fig. 3. The wavelength profile of the sun's Lyα line at 1 AU from the sun (adapted from Lemaire 1978). The profile is centered around the wavelength 1215.67 Å. Inserted in the figure is the FWHM $\Delta\lambda$ for a Doppler profile corresponding to a gas of temperature 8000 K. The wavelength separation between the two P-states is 0.005 Å.

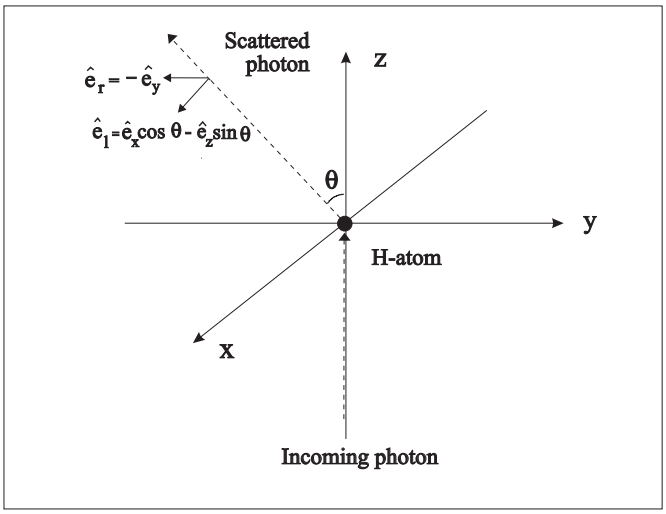

Fig. 4. The definition of the polarization vectors for the scattered light. The scattered beam is taken to lie in the xz-plane.

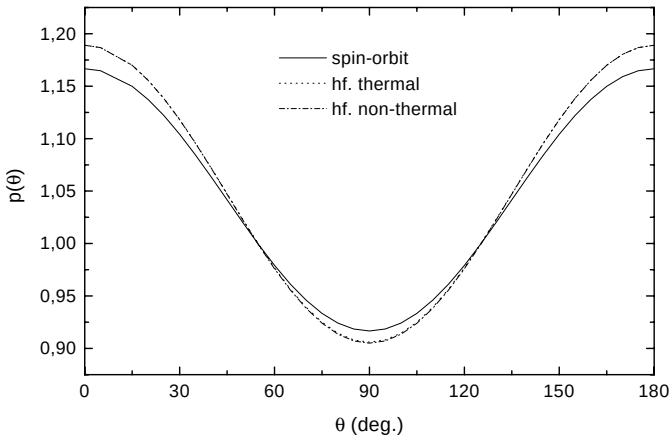

Fig. 5. Phase functions for the spin-orbit case (solid), respectively hyperfine case with thermal (dash) and non-thermal (dot) populations. The difference between the latter two is too small to be discerned clearly in the graph.

These two conditions hold true for the important case of Lyα light from the sun scattered by interstellar hydrogen (see Fig. 3). A direct consequence of criteria 1 and 2 is that the flux $\phi_0(\omega)$ remains constant over the range in which $F(\mathbf{v}, s)$ and the Lorentzian line profile vary. The flux can thus be treated as a constant in the **v**-integration.

3.1. Spin-orbit interaction

To perform the integration over the velocity distribution we start by separating **v** into components parallel and perpendicular to the incoming light direction **q**: $F(\mathbf{v}, s) = F(\mathbf{v}_\parallel, \mathbf{v}_\perp, s)$. Neglecting hyperfine interaction we can divide the sum over intermediate states m into two parts. The first sum will go over the m_J-levels of the $2P_{1/2}$-state and the second sum over the m_J-levels of the $2P_{3/2}$-state. Squaring the term containing the two sums we obtain two quadratic and two cross terms. The denominators can be removed outside the sum as the decay rate Γ_m and frequency separation ω_{mi} will be independent of m. By criterion 2 the function of the parallel velocity component will behave as delta functions in the integration. The cross terms will turn out to be smaller in magnitude by a factor

$$\frac{1}{1+\left(\frac{\omega_{mi}-\omega_{ni}}{\Gamma}\right)^2}\,, \tag{8}$$

as compared to the quadratic terms (m and n refer to the two different P-states). Because $\omega_{ni} - \omega_{mi} = 3.46 \cdot 10^{10}\mathrm{s}^{-1}$ and $\Gamma = 6.257 \cdot 10^8 \mathrm{s}^{-1}$ the cross terms will be a factor 10^{-4} smaller. This approximation is equivalent to treating the different P-states as non-interfering. Inserting the result of the integration

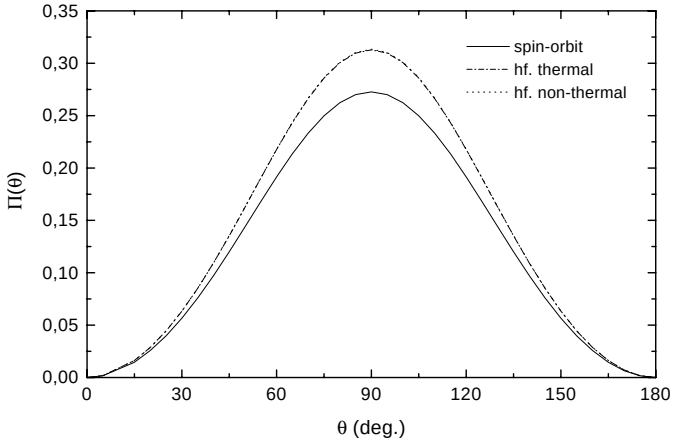

Fig. 6. Polarization functions for the spin-orbit case (solid), hyperfine case, with thermal populations (dash), and for non-thermal populations (dot). Again the difference between the latter two is too small to be discerned.

into Eq. (7) the photon count rate becomes

$$I\ (\omega_{\mathbf{q}}) = \frac{2\pi\alpha^2\omega_{\mathbf{q}}^3\phi_0 r_0^2}{c\,\Gamma} d\omega_{\mathbf{q}} d\Omega\ dA \int ds \frac{n(s)}{r(s)^2} \int d\mathbf{v}_\perp$$
$$F\left(\Lambda_{\mathbf{q}}, \mathbf{v}_\perp, s\right) \sum_{i,f} \left(\left| \sum_m S_m^{if} \right|^2 + \left| \sum_n S_n^{if} \right|^2 \right) \rho_{ii}\,, \qquad (9)$$

where $\Lambda_{\mathbf{q},m} = c((\omega_{\mathbf{q}} - \omega_{mi})/\omega_{\mathbf{q}})$, and by criteria 2 we set $F(\Lambda_{\mathbf{q},m}, \mathbf{v}_\perp, s) = F(\Lambda_{\mathbf{q},n}, \mathbf{v}_\perp, s) \equiv F(\Lambda_{\mathbf{q}}, \mathbf{v}_\perp, s)$. In order to keep the notation compact we have denoted the dipole matrix elements by S_m^{if} and S_n^{if}.

Next we define the scattering geometry. We take the incoming light to define the z-axis, the scattered light to define the xz-plane, and the angle between the scattered light and the z-axis to be θ (see Fig. 4). A convenient choice for the two independent polarization vectors of the incoming light are

$$\hat{e}_+ = \frac{\hat{e}_x + i\hat{e}_y}{\sqrt{2}}$$
$$\hat{e}_- = \frac{\hat{e}_x - i\hat{e}_y}{\sqrt{2}} \qquad (10)$$

and for the scattered light

$$\hat{e}_r = -\hat{e}_y$$
$$\hat{e}_l = \cos\theta\ \hat{e}_x - \sin\theta\ \hat{e}_z\,. \qquad (11)$$

Inserting the relevant dipole matrix elements (see for instance Bethe & Salpeter 1977) and summing over all polarization directions, Eq. (9) gives

$$I(\omega_{\mathbf{q}}) = \frac{2\pi\alpha^2 R^4\omega_{\mathbf{q}}^3\phi_0 r_0^2}{c\,\Gamma} d\omega_{\mathbf{q}} d\Omega\ dA \int ds \frac{n(s)}{r(s)^2}$$
$$\int d\mathbf{v}_\perp F\left(\Lambda_{\mathbf{q}}, \mathbf{v}_\perp, s\right) \frac{1}{81}(14 - 6\sin^2\theta(s)\rho_{22})\,, \qquad (12)$$

where $R = (24/\sqrt{6})(2/3)^5 a_0$ (a_0 being the Bohr radius) is the radial part of the dipole matrix element and the level index i is chosen to coincide with the energy ordering of the levels (for degenerate levels the order is that given by the Zeeman effect). The intensity given by Eq. (12) contains information about the column density of hydrogen atoms. We also see that the parallel component of the velocity distribution is mapped onto the frequency profile of the scattered light. This makes it possible to determine the parallel velocity component from the spectrum. If measurements of the same scattering region could be done from different directions, the three dimensional velocity profile could in principle be reconstructed.

3.2. Hyperfine interaction

If we include hyperfine interaction the sum over intermediate states can be separated into four parts, where each sum goes over the m_F-levels of one F-state (Fig. 2). Squaring we will obtain cross terms containing dipole matrix elements representing scattering via different P-states. These terms can, as before, be neglected. However, terms containing matrix elements representing the scattering via two adjacent hyperfine states must be retained, as Γ and the frequency separation between the F-states are of the same order of magnitude. With this in mind we retrace the steps that lead to Eq. (12) and obtain

$$I\ (\omega_{\mathbf{q}}) = \frac{2\pi\alpha^2 R^4\omega_{\mathbf{q}}^3\phi_0 r_0^2}{c\,\Gamma} d\omega_{\mathbf{q}} d\Omega\ dA \int ds\ \frac{n(s)}{r(s)^2} \int d\mathbf{v}_\perp$$
$$F\left(\Lambda_{\mathbf{q}}, \mathbf{v}_\perp, s\right) \frac{1}{162}\Bigg(22 + 3\rho_{33} + (6 - 9\rho_{33})\cos^2\theta(s) +$$
$$\frac{(4 + 4\cos^2\theta(s))(\rho_{22} + \rho_{44})}{1 + (\frac{2\pi\Delta_1}{\Gamma})^2} - \frac{(3 - 9\cos^2\theta(s))\rho_{33}}{1 + (\frac{2\pi\Delta_2}{\Gamma})^2} \Bigg), \qquad (13)$$

where Δ_1 and Δ_2 are the frequency separation between the hyperfine levels of the $2P_{1/2}$ and $2P_{3/2}$ state, respectively.

3.3. Maxwellian velocity distribution

Next we evaluate Eqs. (12) and (13) for the important special case of an Maxwellian velocity distribution. Assuming that the distribution does not depend on the position of the scattering atom s, we have

$$F(\mathbf{v}) = \left(\frac{m_H}{2\pi k_B T} \right)^{3/2} e^{-\frac{m_H v^2}{2k_B T}}\,, \qquad (14)$$

where m_H is the mass of the hydrogen atom. Inserting Eq. (14) into Eqs. (12) and (13) the velocity integral can be performed analytically, giving

$$I(\omega_{\mathbf{q}}) = \frac{\sqrt{2\pi m_H}\ \alpha^2 R^4\omega_{\mathbf{q}}^3\phi_0 r_0^2}{c\,\Gamma\sqrt{k_B T}} d\omega_{\mathbf{q}} d\Omega\ dA\ e^{-\frac{m_H \Lambda_{\mathbf{q}}^2}{2k_B T}}$$
$$\int ds\ \frac{n(s)}{r(s)^2}\,\overline{p}(\theta(s))\,, \qquad (15)$$

where the two different angular dependent terms have been denoted by $\overline{p}(\theta)$ (this is the non-normalized phase function). To

evalute the LOS integral we need to know the density variations $n(s)$ as a function of s. However, this density information is usually one of the things we want to obtain from our measurements, so we need an initial guess for the distribution. As an intensity measurement in one direction will only give the column density of the hydrogen gas, we will replace $n(s)$ by an average $\langle n(s)\rangle = n$. We can then evaluate the LOS integral analytically by using (see Fig. 4)

$$r^2(s) = r_0^2 \sin^2\theta_0 + (r_0\cos\theta_0 - s)^2$$
$$\cos^2\theta(s) = \frac{(r_0\cos\theta_0 - s)^2}{r_0^2\sin^2\theta_0 + (r_0\cos\theta_0 - s)^2}. \quad (16)$$

The numerical result of the integration will depend on the level structure and the relevant ground state populations.

3.4. Populations

We see from Eqs. (12) and (13) that the scattered intensity depends on the ground state populations. If the hydrogen gas is in thermal equilibrium all the ground states will be equally populated even at very low temperatures (the separation between the F=0 and F=1 state corresponds to a temperature of 0.07 K). This implies that $\rho_{11} = \rho_{22} = 1/2$ in Eq. (12), and $\rho_{11} = \rho_{22} = \rho_{33} = \rho_{44} = 1/4$ in Eq. (13). The above result applies to a gas in which the collision rate exceeds all radiative induced transition rates. There are situations, however, where this no longer is true. In the local interstellar medium, which has a temperature of 8000 K and a density of 0.1 hydrogen atoms per cm^3, the H-H collision rate is 10^{-9}s^{-1}. Other mechanisms which could change the ground state population are charge exchange collisions with solar wind protons and electrons. The rate of both these processes are of the order $10^{-7} - 10^{-8}$s^{-1} at 1 AU (all data are from Holzer 1977). These rates are to be compared to the Lyα induced transition rate which for a flux of $3 \cdot 10^{11}$ cm $^{-2}$ Å^{-1} at 1 AU from the sun (Lemaire et al. 1978) is 10^{-3} s $^{-1}$. We thus see that the ground state population for the hydrogen atoms are determined by the light field.

To determine the populations established by the radiation field we should consider the contribution made by all Lyman series transitions. However, Field (1958) and Varshalovich (1967) have shown that for a constant spectrum the Lyα transition will play the decisive role. This is even more so in the case of the sun as its Lyα intensity is approximately 100 times greater than its Lyβ intensity (Lemaire et al. 1978). Thus the populations established by the Lyα light are the solutions to following set of balance equations

$$\rho_{ii} \sum_f \overline{W}_{i\to f} = \sum_f \rho_{ff} \overline{W}_{f\to i}\,, \quad (17)$$

where $\overline{W}_{i\to f}$ is obtained from W_t by integrating Eq. (4) over all scattering angles. Assuming unpolarized, broad band light, the populations for the spin-orbit case equals

$$\rho_{11} = \rho_{22} = 1/2\,, \quad (18)$$

while for the hyperfine case we get

$$\rho_{11} = \frac{5-G}{21-5G}\ ,\ \rho_{22,44} = \frac{6-2G}{21-5G}\ ,\ \rho_{33} = \frac{4}{21-5G}\,, \quad (19)$$

where $G = 1/(1 + (2\pi\Delta_2/\Gamma)^2) \approx 0.946$ is a measure of the overlap between the F=1 and F=2 levels.
We can estimate the size of the region around the sun in which these populations should dominate. Assuming the H-H collision rate to be independent of the distance from the sun, while the photon scattering rate and charge exchange collision rates varies as the inverse distance squared, we obtain a spherical region of radius $\leq 10^3$ AU in which the radiation is the dominating effect. Two things can be pointed out in connection with Eqs. (18) and (19). The first is that the populations have been calculated assuming the incoming light to be unpolarized. The generalization to other polarization states is done by choosing an appropriate set of polarization vectors, replacing those given in Eq. (10). Varshalovich (1967) treats this more general case, and also considers the effects of 21-cm radiation on the populations. The second point is that Eq. (19) shows that we have a population inversion for the F=1, $m_F = \pm 1$ level. For the sun the region of population inversion is too small to be of any significance in amplifying the 21-cm radiation, but for some O-type stars the region could be large enough to give a measurable maser effect.

3.5. Phase and degree of polarization functions

It is customary in the literature on resonance scattering to give the angular variation of the scattered intensity, or the phase function (Brandt & Chamberlain 1959; Chamberlain 1990). The connection between our results and these phase functions, is obtained by setting $n(s) = \delta(s - s_0)$ in Eqs. (12) and (13), and using the definition

$$p(\theta) = \frac{I(\theta)}{\langle I(\theta)\rangle}\,, \quad (20)$$

where the brackets refer to an integration over all angles and dividing with the total solid angle 4π. Another quantity of interest is the degree of polarization caused by the scattering. This quantity is defined by

$$\Pi(\theta) = \frac{I_r(\theta) - I_l(\theta)}{I_r(\theta) + I_l(\theta)}\,, \quad (21)$$

where the scattered intensity is divided into components along the two polarization vectors in Eq. (11).

Inserting the relevant populations we obtain for the spin-orbit case

$$p(\theta) = \frac{11}{12} + \frac{3}{12}\cos^2\theta \ = \ 0.917 + 0.25\,\cos^2\theta \quad (22)$$

and

$$\Pi(\theta) = \frac{\sin^2\theta}{\frac{11}{3} + \cos^2\theta} \ = \ \frac{\sin^2\theta}{3.667 + \cos^2\theta}\,, \quad (23)$$

Table 1. Phase functions and degree of polarization

Level structure	Polarization	Phase function
Spin-orbit		
thermal pop.	$\frac{\sin^2\theta}{\frac{11}{3}+\cos^2\theta}$	$\frac{11}{12}+\frac{3}{12}\cos^2\theta$
	$\frac{\sin^2\theta}{3.667+\cos^2\theta}$	$0.917+0.25\cos^2\theta$
non-thermal [a]	same	same
Hyperfine		
thermal pop.	$\frac{\sin^2\theta}{3.197+\cos^2\theta}$	$0.906+0.283\cos^2\theta$
non-thermal [a]	$\frac{\sin^2\theta}{3.191+\cos^2\theta}$	$0.905+0.284\cos^2\theta$

[a] Populations established by light-atom interaction.

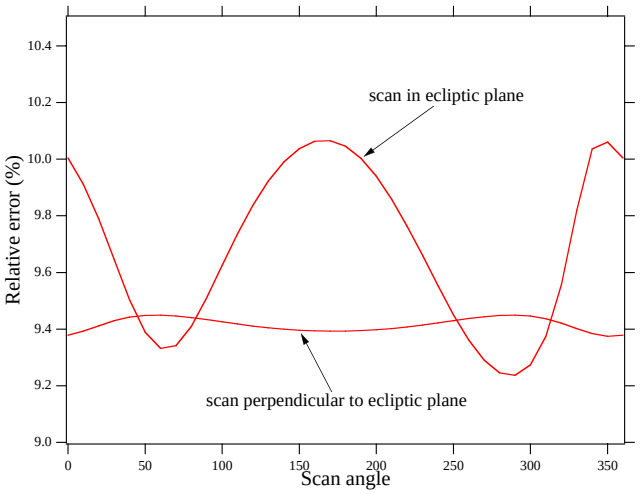

Fig. 7. The relative difference (Δ) in the simulated signals when the two phase functions in Eqs. (22) and (26) are used. Two different geometries are described in the text.

which is in agreement with the formulas given by Brandt & Chamberlain (1959). Similar calculations for the hyperfine case, using thermal populations, give

$$p(\theta) = 0.906 + 0.283\,\cos^2\theta \tag{24}$$

and

$$\Pi(\theta) = \frac{\sin^2\theta}{3.197 + \cos^2\theta}\,. \tag{25}$$

If instead of the thermal populations we use those given by Eq. (19), we get

$$p(\theta) = 0.905 + 0.284\,\cos^2\theta \tag{26}$$

and

$$\Pi(\theta) = \frac{\sin^2\theta}{3.191 + \cos^2\theta}\,, \tag{27}$$

The above results are summarized in Table 1 and compared in Figs. 5 and 6.

Expressions (24) thru (27) have not previously been published. Chamberlain (1990) gives a phase function for the hyperfine case using thermal populations and assuming non-interfering levels which equals

$$p(\theta) = \frac{91}{96} + \frac{15}{96}\cos^2\theta \;=\; 0.948 + 0.156\,\cos^2\theta\,. \tag{28}$$

The validity of this formula is, however, questionable as the interference will introduce a significant correction to the final result.

4. Numerical simulations

To see what difference the level structure makes in the measured intensity, we compare the spin-orbit case, Eq. (12), and the hyperfine case, Eq. (13). Taking for simplicity the homogeneous case $n(s) = n$, we can use the results of Sect. 3.3. The relative intensity difference thus obtained is $I_{so}/I_{hf} = 0.92$ (where we used $r_0 = 1$ AU), implying that the hyperfine case will give an 8 % higher scattered intensity, as compared to the spin-orbit case. Comparing the intensities for the thermal and non-thermal populations of the hyperfine case in a similar way, we will get at difference less than 0.1 %. From the latter comparison we see that the non-thermal populations will not have an effect on the scattered intensity.

In order to see the changes in a more realistic case we use one measurement location of the SOHO spacecraft. SOHO is ESA-NASA spacecraft (launched in December 1995) which carries a Lyman alpha instrument named SWAN (Solar Wind Anisotropies). SWAN is capable to carry out a full sky mapping of Lyman alpha radiation. The data analysis of SWAN has only recently started (see Bertaux et al. 1997 and Kyrölä et al. 1997) and therefore a full comparison between data and models is not possible in this work. In the following we use a realistic description of the velocity distribution of the interstellar hydrogen cloud in the solar neigbourhood. The details of the model are explained in Kyrölä et al. 1997 where it is called the isotropic reference model (the details of the model will not be important in the following analysis). The measurement day is on 5th of March, 1996. The SOHO location is (-0.9710, 0.2389, 0.0006) in ecliptic coordinates and in AU-units. Using this position we perform two simulations. The first simulation consists of a full circle of line of sights in the ecliptic plane (excluding the solar source). The second simulation is a full circle scan perpendicular to the SOHO-Sun line. Because SOHO is very accurately in the ecliptic plane these lines of sights are in the plane perpendicular to the ecliptic plane. The two phase functions we compare are the much used fine structure result of Eq. (22) and the hyperfine structure result of Eq. (26). In the simulation we have used the total scattered intensity, which is obtained from the Eqs. (12) and (13) by integrating over all measured frequencies. The intensity thus obtained is

$$I = \sigma\phi_{0\lambda}r_0^2\int \frac{ds}{r(s)^2} n(\boldsymbol{r}(s))p(\theta(s))\,. \tag{29}$$

The value of the cross section σ in Eq. (29) is different for the spin-orbit and hyperfine case and is given by

$$\sigma_{so} = \frac{e^2 R^2}{6\hbar\epsilon_0}\frac{\lambda_0}{c} \tag{30}$$

and

$$\sigma_{hf} = 0.180 \cdot \frac{e^2 R^2}{\hbar\epsilon_0}\frac{\lambda_0}{c}\ , \tag{31}$$

respectively. The relative error between these two results

$$\Delta = \frac{I_{so} - I_{hf}}{I_{so}}\ , \tag{32}$$

is shown in Fig. 7 for the two scanning geometries just described. It is seen that the error lies between 9.2-10% and thus is somewhat higher than in the constant density case considered first.

5. Conclusions

In this work we have carried out a full quantum mechanical calculation for the Lyα scattering phase and polarization functions. The hyperfine level structure of the hydrogen atom and the populations established by the Lyα light are taken into account. The resulting phase functions, and thus measured intensities, differ in the case of a realistic model for the density $n(s)$ from the widely used fine structure phase function by 10%. This difference is quite large and should thus be detectable in the data. The Lyα mapper SWAN on the SOHO satellite will probably provide data good enough to make a comparisons between the different phase functions possible. However, as many other factors (like multiple scattering and the density distribution used) are also of importance in interpreting the data, this comparison may not be straightforward.

We saw that in order to explicitly evaluate the scattered intensity one needs the frequency profile of the incoming light and the velocity distribution of the atoms. We have throughout been assuming a flat frequency profile, but have not, except in Sect. 3.3., specified the form of the velocity distribution. By measuring the spectrum of the scattered light we can obtain information about the parallel component of the velocity distribution. In the case of a pure Maxwell-Boltzmann distribution this would directly give us the temperature of the scattering gas. For an asymmetric velocity distribution, the spectrum would be smeared out by the LOS integration. In our calculations we have also neglected the effects of multiple scattering. If multiple scattering is of importance our LOS integrals are no longer valid. Keller (1981) have estimated, by using Monte Carlo methods, that the optically thin approximation underestimates the scattered intensity from the nearby interstellar medium by 5 to 35%, depending on the direction of the LOS. Scherer & Fahr (1996) has used a more analytical approach to the multiple scattering problem and taken into account an angle-dependent partial frequency redistribution. As input in their calculations they have used the phase function of Brand and Chamberlain. On the basis of our numerical simulations one would then expect a 10% change in their integrated intensity when using our phase functions. Also the temperature inferred from the line width of the scattered light is effected due to the line broadening caused by the multiple scattering. Quémerais & Bertaux (1993) estimates that temperature is off by about 30 %. Although our LOS integrals are not accurate enough under these circumstances, the phase functions listed in Table 1 will still be useful, as they apply to the scattering from a single atom, and thus can be used as a starting point in the numerical simulations.

Acknowledgements. We would like to thank Markus Lindberg, at the Department of Physics, Åbo Akademi University, for illuminating discussions.We also thank the referee for suggestions to improve this paper.

References

Bertaux J-L., Quemerais E., Lallement R., et al., submitted to Solar Physics, 1997
Bethe H. A., Salpeter E. E., 1977, Quantum mechanics of one- and two-electron atoms, Plenum, New York
Brandt J. C., Chamberlain J. W., 1959, ApJ 130, 670
Breit G., 1933, Rev. Mod. Phys. 5, 91
Chamberlain J. W., 1990, Icarus 84, 106
Field G. B., 1958, Proc. IRE 46, 240
Hamilton D. R., 1947, ApJ 106, 457
Holzer T. E., 1977, Rev. Geophys. SpaceSci. 15, 467
Keller H. U., Richter K., Thomas G. E., 1981, A&A 102, 415
Kyrölä E., Summanen T., Schmidt W., et al., submitted to JGR, 1997
Lemaire P., Charra J., Jouchoux A., et al., 1978, ApJ 223, L55
Louisell W. H., 1973, Quantum Statistical Properties of Radiation, Wiley, New York
Quémerais E., Bertaux J-L., 1993, A&A 277, 283
Scherer K., Fahr H. J., 1996, A&A 309, 957
Varshalovich D. A., 1967, Soviet Phys. JETP 25, 157
Weisskopf V. F., 1931, Ann. d. Phys. 9, 27